IOP Conf. Series: Materials Science and Engineering **225** (2017) 012295 doi:10.1088/1757-899X/225/1/012295

Large Elasto-Plastic Deformations in Bi-Material Components by Coupled FE-EFGM

G. A. Harmain[1], Azher Jameel[2,3], Farooq A. Najar[3], Junaid H. Masoodi[3]

[1]Professor, Department of Mechanical Engineering, National Institute of Technology Srinagar, Hazratbal, 190006, India.

[2]Assistant Professor, Department of Mechanical Engineering, Shri Mata Vaishno Devi University Katra, 182320, India.

[3]Research Scholar, Department of Mechanical Engineering, National Institute of Technology Srinagar, Hazratbal, 190006, India.

Email:jameelazher22@gmail.com

Abstract. In the recent years, the coupled finite element-element free Galerkin method (coupled FE-EFGM) has found wide application in modeling large elasto-plastic deformations in bi-material components. The coupled FE-EFGM applies EFGM in the portion of the domain where large deformations are expected to occur, whereas the rest of the domain is discretized into conventional finite elements. The large deformation occurring in the domain has been modeled by using the total Lagrangian approach. The non-linear elasto-plastic behavior of the material has been represented by the Ramberg-Osgood model. Finally, two numerical problems are solved by the coupled FE-EFGM to illustrate its applicability, efficiency and accuracy in modeling large elasto-plastic deformations in bi-material samples.

Keywords. Bi-material components, Coupled FE-EFGM, Large Deformations.

1. Introduction

The modeling of large deformation in engineering components containing internal material interfaces is very difficult in the conventional finite element method (FEM) because of the need for mesh adaption and conformal meshing [1-3]. The enriched techniques like the coupled FE-EFGM model different types of internal discontinuities independent of the mesh or the grid. FEM faces extreme mesh distortion issues while modeling large elasto-plastic deformations in engineering components due to which the remeshing of domain is required time and again during simulation [4-6]. The coupled FE-EFGM couples the two techniques together and provides a strong numerical tool that exploits the advantages of both FEM and EFGM. The coupled FE-EFGM proves to be a very efficient numerical tool for modeling large elasto-plastic deformations in bi-material engineering components, where large deformations are confined to a portion of the specimen only. EFGM [7-10] is used to discretize the portion of the domain where large elasto-plastic deformations are expected to occur whereas the conventional FEM is used in the rest of the domain. The coupled FE-EFGM proves to a very efficient numerical tool for modeling large elasto-plastic deformations in bi-material engineering specimens. The coupled FE-EFGM was successfully applied for the direct imposition of essential boundary

conditions by Krongauz and Belytschko [11]. Several techniques have been proposed for appropriate coupling between FEM and EFGM [12-13]. The coupled FE-EFGM has been successfully applied to model some simple elastic problems and a few elasto-plastic crack growth problems [14].

The present study models large elasto-plastic deformations in bi-material engineering components by employing the coupled FE-EFGM. The large deformation occurring in the domain has been modeled by the total Lagrangian approach. The nonlinear material behavior has been characterized by the generalized Ramberg-Osgood model. The stresses have been computed by employing the elastic-predictor and plastic-corrector algorithm [15]. The plasticity has been modeled by applying the Von-Mises failure criterion with isotropic strain hardening. The discontinuities present in the domain have been represented by the level set method. Finally, the proposed technique has been used to solve large elasto-plastic deformations in bi-material engineering components subjected to different type of loads.

2. Modeling of Large Deformation

When a body undergoes large deformations, its geometry changes continuously during analysis and the body takes definite configuration after the application of each load step. The deformation of a body is completely defined by the deformation gradient, which relates the deformed state of a particular body with its undeformed state. The deformation gradient (F) giving the relationship between the deformed state and the undeformed state can be defined as $dx = F.dX$, where x denotes the position of the point in the deformed configuration and X denotes the coordinates of the point in the deformed state. In large deformation analysis, two types of strain measures are extensively used. The first one is the Green-Lagrange strain tensor, which describes the change in length with respect to the original undeformed length. The second strain measure is the Almansi-Hamel strain tensor, which describes the change in length with respect to the current deformed configuration. The Cartesian components of the Green strain tensor (E) and the Almansi strain tensor (e) can be written as

$$E_{ij} = \frac{1}{2}\left(\frac{\partial x_m}{\partial X_i}\frac{\partial x_m}{\partial X_j} - \delta_{ij}\right) \;;\; e_{ij} = \frac{1}{2}\left(\delta_{ij} - \frac{\partial X_m}{\partial x_i}\frac{\partial X_m}{\partial x_j}\right) \quad (1)$$

Three types of stress measures are used in large deformation analysis. The first stress measure is the Cauchy stress tensor (σ), which can be defined as the current force acting on the deformed configuration per unit deformed (actual) area. The second stress measure is the first Piola-Kirchhoff stress tensor (P), which may be defined as the force acting on the current deformed configuration per unit original undeformed area. The third stress measure is the second Piola-Kirchhoff stress tensor (S), which is defined as the force acting on the undeformed area per unit undeformed area.

3. Total Lagrangian Formulation

The total Lagrangian approach uses the initial undeformed configuration(C_0), as the reference configuration for analysis. All quantities such as the displacements, stresses and strains are measured with respect to C_0 configuration. The equilibrium equation of a deformable body under the action of external forces can be written as

$$\int_{{}^0\Omega} S_{ij}\,\delta(E_{ij})\,d\,{}^0\Omega - \int_{{}^0\Omega} f_i\,\delta u_i\,d\,{}^0\Omega - \int_{{}^0\Gamma} {}^2_0t_i\,\delta u_i\,d\,{}^0\Gamma = 0 \quad (2)$$

where f represent the body forces, t represents the applied tractions and u denotes the unknown displacements. All quantities are expressed in terms of initial undeformed configuration. In order to develop the numerical model for large deformation analysis, we have to approximate the displacement field. The total and incremental displacement fields can be approximated in FEM or EFGM as

$$\boldsymbol{u}(\boldsymbol{x}) = \sum_{i=1}^{n} \Psi_i(\boldsymbol{x})\boldsymbol{u}_i \quad (3)$$

where $\boldsymbol{u} = [uv]^T$, $\boldsymbol{u}_i$denotes the standard degrees of freedom and n denotes the number of present in the domain. $\Psi_i$represents the interpolation or shape functions. In FEM, $\Psi_i$represents the conventional finite element Lagrange shape functions whereas Ψ_i represents the MLS shape functions in EFGM. The approximate solution can be written in matrix form as $\{\boldsymbol{u}\} = [\boldsymbol{\Psi}]\{\boldsymbol{\Delta}\}$, where $\{\boldsymbol{\Delta}\} = [u_i v_i]^T$,

$[\boldsymbol{\Psi}] = \begin{bmatrix} \Psi_i & 0 \\ 0 & \Psi_i \end{bmatrix}$. After making appropriate substitutions in the equilibrium equation, we obtain the final numerical model for total Lagrangian approach as $[\mathbf{K}]\{\boldsymbol{\Delta}\} = \{\boldsymbol{f}\}$ such that

$$\boldsymbol{K} = \int_{{}^0\Omega} [\boldsymbol{B}]^T [\boldsymbol{C}][\boldsymbol{B}] \, \mathrm{d}\, {}^0\Omega + \int_{{}^0\Omega} [\mathbf{G}]^T [\boldsymbol{M_S}][\mathbf{G}] \, \mathrm{d}\, {}^0\Omega \tag{4}$$

$$\boldsymbol{f} = \int_{{}^0\Omega} [\boldsymbol{\Psi}]^T \{\boldsymbol{f}\} \, \mathrm{d}\, {}^0\Omega + \int_{{}^0\Gamma} [\boldsymbol{\Psi}]^T \{\boldsymbol{t}\} \, \mathrm{d}\, {}^0\Gamma - \int_{{}^0\Omega} [\mathbf{B}]^T \{\boldsymbol{S}\} \, \mathrm{d}\, {}^0\Omega \tag{5}$$

$$[\mathbf{B}] = [\mathbf{D}][\boldsymbol{\Psi}] \quad ; \quad [\mathbf{G}] = [\overline{\mathbf{D}}][\boldsymbol{\Psi}] \tag{6}$$

$$\{\boldsymbol{f}\} = \begin{bmatrix} \boldsymbol{f}_x \boldsymbol{f}_y \end{bmatrix}^T \quad ; \quad \{\boldsymbol{t}\} = \begin{bmatrix} \boldsymbol{t}_x \boldsymbol{t}_y \end{bmatrix}^T \tag{7}$$

$$[\mathrm{D}] = \begin{bmatrix} \left(1 + \frac{\partial u}{\partial x}\right)\frac{\partial}{\partial x} & \frac{\partial v}{\partial x}\frac{\partial}{\partial x} \\ \frac{\partial u}{\partial y}\frac{\partial}{\partial y} & \left(1 + \frac{\partial v}{\partial y}\right)\frac{\partial}{\partial y} \\ \left(1 + \frac{\partial u}{\partial x}\right)\frac{\partial}{\partial y} + \frac{\partial u}{\partial y}\frac{\partial}{\partial x} & \left(1 + \frac{\partial v}{\partial y}\right)\frac{\partial}{\partial x} + \frac{\partial v}{\partial x}\frac{\partial}{\partial y} \end{bmatrix} ; \; [\overline{D}] = \begin{bmatrix} \frac{\partial}{\partial x} & 0 \\ \frac{\partial}{\partial y} & 0 \\ 0 & \frac{\partial}{\partial x} \\ 0 & \frac{\partial}{\partial y} \end{bmatrix} \tag{8}$$

$$\{\mathbf{E}\} = \begin{Bmatrix} S_{xx} S_{yy} S_{xy} \end{Bmatrix}^T = [\mathbf{C}]\{\boldsymbol{E}\} \tag{9}$$

$$\{\boldsymbol{E}\} = \begin{Bmatrix} E_{xx} E_{yy} & 2E_{xy} \end{Bmatrix}^T = \begin{Bmatrix} \frac{\partial u}{\partial x} + \frac{1}{2}\left(\frac{\partial u}{\partial x}\right)^2 + \frac{1}{2}\left(\frac{\partial v}{\partial x}\right)^2 \\ \frac{\partial v}{\partial y} + \frac{1}{2}\left(\frac{\partial u}{\partial y}\right)^2 + \frac{1}{2}\left(\frac{\partial v}{\partial y}\right)^2 \\ \frac{\partial v}{\partial x} + \frac{\partial u}{\partial y} + \frac{\partial u}{\partial x}\frac{\partial u}{\partial y} + \frac{\partial v}{\partial x}\frac{\partial v}{\partial y} \end{Bmatrix} \tag{10}$$

$$[M_S] = \begin{bmatrix} S_{xx} & S_{xy} & 0 & 0 \\ S_{xy} & S_{yy} & 0 & 0 \\ 0 & 0 & S_{xx} & S_{xy} \\ 0 & 0 & S_{xy} & S_{yy} \end{bmatrix} \tag{11}$$

4. Coupling Between FEM and EFGM

The Coupled FE-EFGM employs EFGM in the region where large elasto-plastic deformations occur and the rest of the domain is discretized into conventional finite elements. The FE region and EFG region are coupled together by introducing interface or transition elements between FE nodes and EFG nodes. The whole domain (Ω)is divided into three separate sub-domains like the FE region (Ω^{FE}), the EFG region (Ω^{EFG}) and the transition region (Ω^{TE}). The displacement approximation in the FEM region can be written as

$$u(\boldsymbol{x}) = \sum_{i=1}^{\boldsymbol{n}} \mathrm{N}_i(\boldsymbol{x})\, u_i \quad ; \quad \boldsymbol{x} \in \Omega^{\mathrm{FE}} \tag{12}$$

where$\mathrm{N}_i(\boldsymbol{x})$denotes the finite element shape functions, n the number of nodes and $u_i$the nodal degrees of freedom. In the EFGM region, the displacement approximation can be written as

$$u(\boldsymbol{x}) = \sum_{j=1}^{\boldsymbol{n}} P_j(\boldsymbol{x})\, a_j(\boldsymbol{x}) = \boldsymbol{P}^T(\boldsymbol{x})\boldsymbol{a}(\boldsymbol{x}) = \boldsymbol{\Psi}(\boldsymbol{x})\boldsymbol{u} \quad ; \quad \boldsymbol{x} \in \Omega^{\mathrm{EFG}} \tag{13}$$

where$\boldsymbol{P}^T(\boldsymbol{x})$ represents a matrix of polynomial basis functions, n is the order of the basis function, and $\boldsymbol{a}(\boldsymbol{x})$denotes a matrix of unknown coefficients. '$\boldsymbol{\Psi}$ ' represents a matrix of MLS shape functions used in EFGM and can be written as

$$\boldsymbol{\Psi}(\boldsymbol{x}) = \mathbf{P}^T(\boldsymbol{x})\mathbf{A}^{-1}(\boldsymbol{x})\mathbf{B}(\boldsymbol{x}) \tag{14}$$

where

$$\mathbf{A}(\boldsymbol{x}) = \sum_{j=1}^{n} w_j(\boldsymbol{x})\mathbf{P}(\boldsymbol{x}_j)\mathbf{P}^T(\boldsymbol{x}_j) \tag{15}$$

$$\mathbf{B}(\boldsymbol{x}) = [w_1(\boldsymbol{x})\mathbf{P}(\boldsymbol{x}_1),\ w_2(\boldsymbol{x})\mathbf{P}(\boldsymbol{x}_2), \ldots\ldots\ldots, w_n(\boldsymbol{x})\mathbf{P}(\boldsymbol{x}_n)] \tag{16}$$

The displacement approximation across the transition element is obtained by employing the Ramp function. The displacement approximation across the transition element can be written as

$$u(\boldsymbol{x}) = [1 - R(\boldsymbol{x})]\boldsymbol{u}^{FE}(\boldsymbol{x}) + R(\boldsymbol{x})\boldsymbol{u}^{EFG}(\boldsymbol{x}) \tag{17}$$

where$R(\boldsymbol{x})$ is the Ramp function which varies linearly from zero at the finite element boundary to one at the meshfree boundary. $\boldsymbol{u}^{FE}$denotes the FEM approximation and $\boldsymbol{u}^{EFG}$represents the EFGM approximation. For numerical calculations, the Ramp function can be obtained as

$$R(\boldsymbol{x}) = \sum_{j=1}^{\boldsymbol{n_e}} \mathrm{N}_j(\boldsymbol{x}) \tag{18}$$

where, $\boldsymbol{n_e}$denotes the number of nodes lying on the meshfree boundary of the interface or transition element. Now, the displacement approximation for transition elements can be written as

$$\boldsymbol{u}(\boldsymbol{x}) = \sum_{i=1}^{\boldsymbol{n_E}} \widetilde{\boldsymbol{\Psi}}_{\boldsymbol{i}}(\boldsymbol{x})\boldsymbol{u}_i \tag{19}$$

where, $\widetilde{\boldsymbol{\Psi}}_{\boldsymbol{i}}$ denotes the shape functions for interface elements, which can be written as

$$\widetilde{\boldsymbol{\Psi}}_{\boldsymbol{i}}(\boldsymbol{x}) = \begin{cases} [1 - R(\boldsymbol{x})]\boldsymbol{N_i}(\boldsymbol{x}) + R(\boldsymbol{x})\boldsymbol{\Psi_i}(\boldsymbol{x}) & ; \quad \boldsymbol{x} \in \Omega^{\mathrm{TE}} \\ R(\boldsymbol{x})\boldsymbol{\Psi_i}(\boldsymbol{x}) & ; \quad \boldsymbol{x} \notin \Omega^{\mathrm{TE}} \end{cases} \tag{20}$$

5. Numerical Results and Discussions

Now, we present two numerical problems involving large elasto-plastic deformations in bi-material specimens that were solved by coupled FE-EFGM. The total Lagrangian approach has been used to model the large deformations occurring in the domain. The grid size of 26×41 nodes has been considered for analysis. The coupled FE-EFG method provides an efficient numerical tool for modeling large deformation in bi-material samples, where large deformations are confined to the weak portion of the specimen only. The weaker portion of the domain is analyzed by EFGM, whereas the remaining portion of the domain is discretized into conventional finite elements. Thus, we are able to take advantage of both the numerical techniques. The results obtained by the coupled FE-EFGM are compared with XFEM and EFGM results, which have been taken as the reference solution for the given problems.

5.1. Large Deformation with Horizontal Bi-material Interface

The large elasto-plastic deformation in a rectangular component with a horizontal bi-material interface is presented here. A rectangular plate $(4\ cm \times 6\ cm)$is fixed at the top edge and a uniform compaction displacement of $1\ cm$ height reduction is imposed at the bottom edge, as shown in Fig. 1. The weaker portion of the specimen is assumed to exhibit the elasto-plastic behavior with the Young's modulus of $2.1 \times 10^{10} N/m^2$, Poisson's ratio of 0.35, yield stress of $2.4 \times 10^{8} N/m^2$and a hardening parameter of $3.0 \times 10^{9} N/m^2$. The stronger portion of the domain is assumed remain elastic during simulation, with the Young's modulus of $2.1 \times 10^{11} N/m^2$, Poisson's ratio of 0.35. The domain representation of the given bi-material sample in coupled FE-EFGM is shown in Fig. 2(a). The deformed configuration corresponding to the compaction of $1\ cm$ is shown in Fig. 2(b). The variations of the normal stresses along the bi-material interface and the bottom edge are shown in Fig. 3. The results show that the proposed numerical technique can be efficiently and accurately applied to solve large elasto-plastic deformations in different engineering components containing bi-material interfaces. The results obtained by the coupled FE-EFGM show a remarkable agreement with the results obtained by XFEM and EFGM.

5.2. Large Deformation with Two Horizontal Bi-material Interfaces

The large elasto-plastic deformation in a rectangular component $(4\ cm \times 6\ cm)$ with two horizontal bi-material interfaces is presented here. The plate is fixed at the top edge and a uniform compaction displacement of $7.5\ mm$ is imposed at the bottom edge, as shown in Fig. 1. The material properties of the weaker and stronger portion are assumed to be the same as in the previous case. The domain representation of the given rectangular specimen with two bi-material interfaces is shown in Fig. 4(a). The deformed configuration corresponding to the compaction of $7.5\ mm$ is shown in Fig. 4(b). The variations of the normal stresses along the bi-material interface and bottom edge are shown in Fig. 5. The coupled FE-EFGM provides a better framework for modeling large deformation problems, because it utilizes the advantages of both FEM and EFGM during simulation.

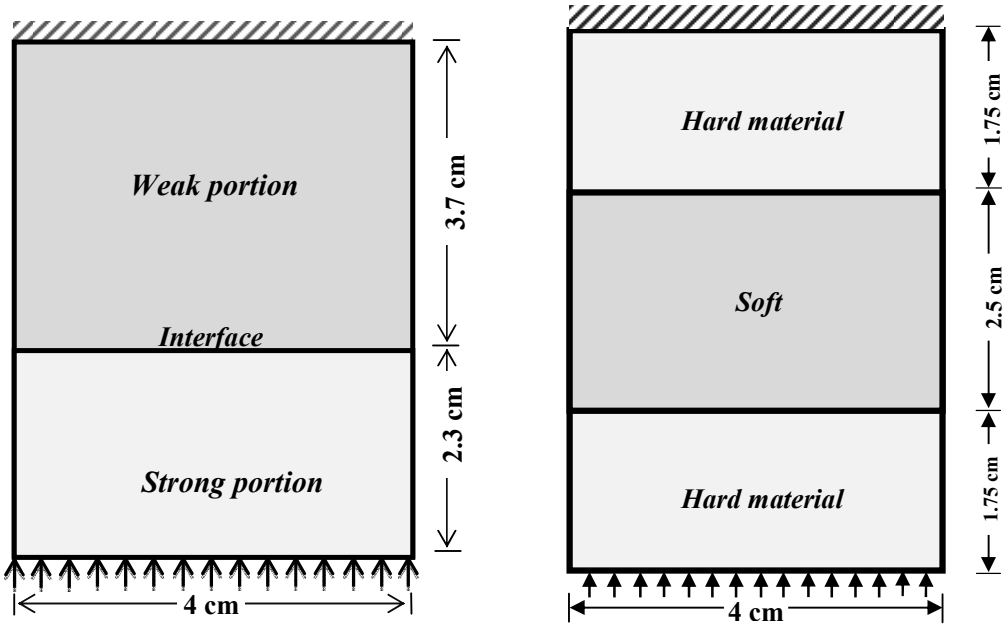

Fig. 1: Rectangular component with bi-material interfaces.

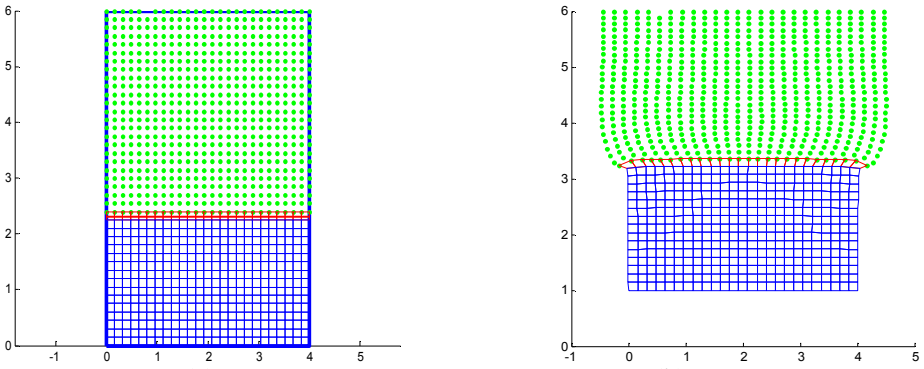

(a) (b)

Fig. 2: Rectangular component with one bi-material interface. (a) Domain representation (b) Deformed shape

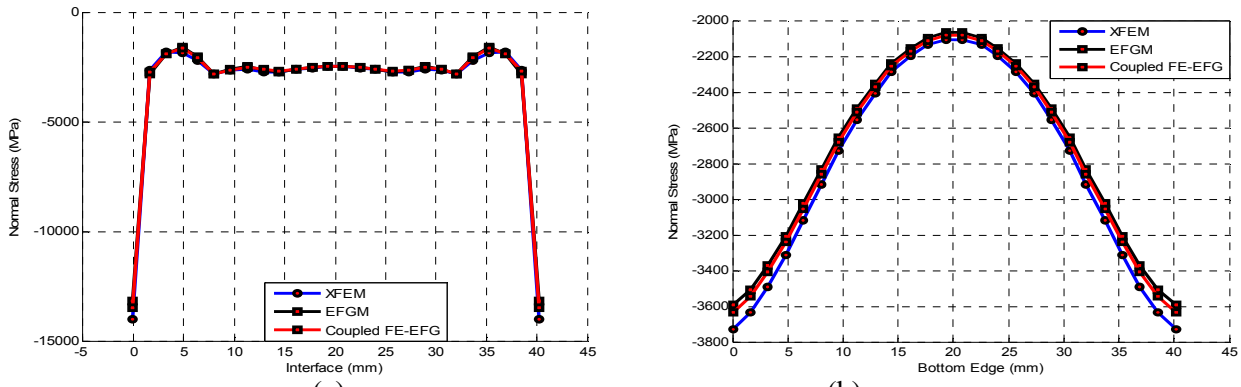

(a) (b)

Fig. 3: Variation of Normal stress (a) Along bi-material interface (b) Along bottom edge.

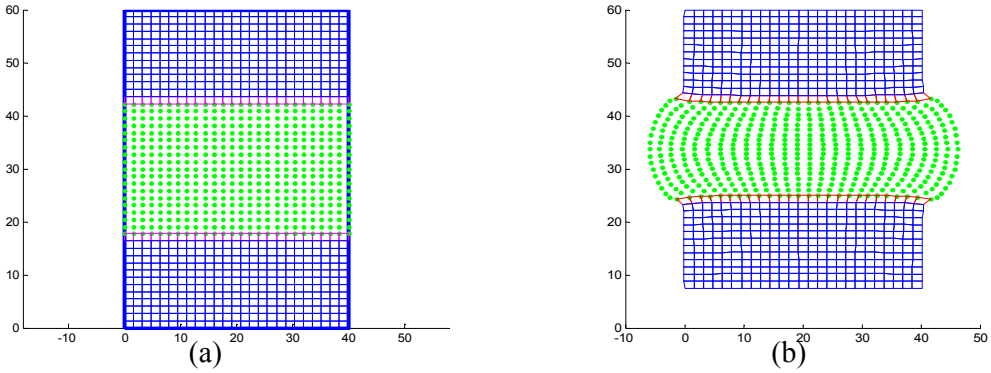

Fig. 4: Rectangular component with two bi-material interfaces. (a) Domain representation (b) Deformed shape.

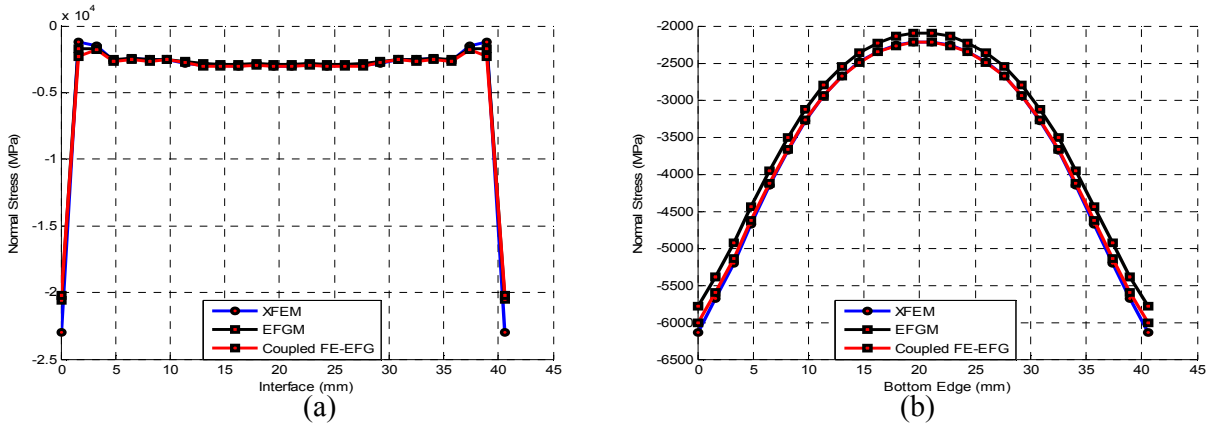

Fig. 5: Variation of Normal stress (a) Along bi-material interface(b) Along bottom edge.

6. Conclusions

The present work employs coupled FE-EFGM for modeling large elasto-plastic deformations in bi-material engineering components. The coupled FE-EFGM exploits the advantages of both FEM and EFGM and provides a strong numerical tool for modeling large elasto-plastic deformations in bi-material specimens, where large deformations are confined to a portion of the domain only. The results obtained by coupled FE-EFGM show a remarkable agreement with the results obtained by XFEM and EFGM. The results also show the capabilities of the coupled FE-EFGM in modeling large elasto-plastic deformations in bi-material engineering components.

References

[1] Cheung S and Luxmoore AR 2003 *Engrng. Fract. Mech.***70** 1153–69
[2] Singh IV, Mishra BK, Bhattacharya S and Patil RU 2012 *Int. J. Fatigue***36** 109–19
[3] Jameel A and Harmain GA 2016 *Streng. Mater.***48** 294–306
[4] Portela A, Aliabadi M and Rooke D 1991 *Int. J. Numer. Meth. Engrng*. **33** 1269–87
[5] Yan AM and Nguyen-Dang H 1995 *Comput. Mech.***16** 273–80
[6] Yan X 2006 *Mech. Res. Commun*. **33** 470–81
[7] Pant M, Singh IV and Mishra BK 2010 *Int. J. Mech. Sci*. **52** 1745–55
[8] Belytschko T, Lu YY and Gu L 1995 *Engrng. Fract. Mech.* **51** 295–315
[9] Duflot Mand Nguyen-Dang H 2004 *Int. J. Numer. Meth. Engrng.* **59** 1945–61
[10] Duflot Mand Nguyen-Dang H 2004 *J. Comput. Appl. Mech*. **168** 155–64

[11] Nayroles B, Touzot G and Villon P 1992 *Comput. Mech.***10** 307-18
[12] Hegen D 1996 *Comp. Methods Appl. Mech. Engrng*. **135** 143–66
[13] Karutz H, Chudoba R and Kratzig WB 2002 *Finite Elem. Anal. Des*. **38** 1075–91
[14] Kumar S, Singh IV and Mishra BK 2014 *Theoret. Appl. Fract. Mech.***70** 49-58
[15] Jameel A and Harmain GA 2015 *Int. J. Fatigue***81** 105-16